Novel production method for traceable surface sources by aluminium functionalisation

Dilan Tuzun, Lucille Chambon, Yann Kergadallan, Valérie Lourenço

Applied Radiation and Isotopes 202 (2023) 111045

Contents lists available at ScienceDirect

Applied Radiation and Isotopes

journal homepage: www.elsevier.com/locate/apradiso

Novel production method for traceable surface sources by aluminium functionalisation

D. Tüzün, L. Chambon, Y. Kergadallan, V. Lourenço *

Université Paris-Saclay, CEA, List, Laboratoire National Henri Becquerel (LNE-LNHB), F-91120, Palaiseau, France

ARTICLE INFO

Keywords:
Radioactive source
Large area surface sources
Surface functionalisation
Eu-152
Am-241

ABSTRACT

Accurate detection of low-level radioactivity is critical in decommissioning. However, commercial sources used for calibration lack representativeness due to their flat surface. The objective of this work is to produce flexible and large area surface sources for alpha and beta emitters by functionalising aluminium foil. Functionalisation strategies were developed to provide these sources. The manganese oxide coated sample shows the highest fixation yield for ^{241}Am: (70.0 ± 2.6)% and conforms to ISO 8769 for uniformity (92%).

1. Introduction

Decommissioning of nuclear facilities is a complex and challenging process that requires careful planning and execution to ensure the safety of workers and the surrounding community. One of the most important steps in decommissioning is the accurate classification of potential waste based on the level of radioactivity. This process involves differentiating non-contaminating surfaces from low-level contaminated surfaces, following specific threshold values, for example 0.2 Bq•cm^{-2} in France (Chambon et al., 2022). This requires an accurate mapping of all surfaces, a task that becomes even more challenging when dealing with non-flat surfaces such as pipes and other complex shapes.

Calibration of contamination detectors is required to ensure accurate measurements. However, commercial calibration sources composed of rigid aluminium (Al, 3 mm thick) are limited in terms of their representativeness and size (150 cm^2). Our objective is to provide non-contaminating surfaces and replicate complex shapes, thereby enabling the assessment of measurement biases and providing a reliable calibration.

These sources can be produced using a variety of substrates (Chambon et al., 2022), but we focused on Al foils to benefit from a possible comparison with existing thicker commercial sources. In addition, Al offers advantages such as conductivity, low cost, easy availability, and potentially high surface area.

The chosen approach to produce surface sources relies on introducing new functional group onto Al foils that can chemically bind to radionuclides (RN). The intent behind this method is to attach the radionuclides predominantly to the surface of the substrate, thereby minimising the penetration and self-absorption of the alpha and beta radiation. Additionally, this technique should involve the formation of strong chemical bonds between the RNs and the Al surface. Consequently, unlike commercial sources, these sources can be a new way to obtain non-contaminating sources. By limiting the self-absorption of radiation and eliminating the need for protective layers, these sources offer a non-contaminating alternative that can help mitigate the risks associated with calibrating and checking the instruments on-site.

To immobilise RNs on the surface of Al foil, three distinct methods for functionalising were studied: sulfonation, manganese oxide coating and chromium oxide coating. These functionalisation methods draw inspiration from literature on enhancing hydrophilicity and implementing anti-corrosion coatings for Al (Chen et al., 2010; Kulinich and Akhtar, 2012).

The first method, sulfonation, involves introducing sulfonic acid functional groups to an Al substrate to immobilise RNs, such as Am^{3+}or $[UO_2]^{2+}$, on the surface by cation exchange. This method was adapted from a porous anodic Al membrane modification method to change its surface charge (Chen et al., 2010). The second and third methods involve coating the Al with a layer that acts as a cation exchanger. These methods are primarily used to improve the optimal adhesion capabilities and corrosion performance (del Olmo et al., 2022; Kulinich and Akhtar, 2012; Siau et al., 2004). The second method, manganese treatment, involves the reduction of Mn(VII) to a lower state, followed by precipitation as an oxide layer that coats and passivates Al (Kulinich and Akhtar, 2012). This reaction generally involves a basic medium during

* Corresponding author.
E-mail address: valerie.lourenco@cea.fr (V. Lourenço).

https://doi.org/10.1016/j.apradiso.2023.111045
Received 20 June 2023; Received in revised form 26 August 2023; Accepted 22 September 2023
Available online 23 September 2023

functionalisation. A method with chromium, taking place at acidic pH (Siau et al., 2004), was implemented to compare the effect of pH of the functionalisation step on RN binding experiments. The chromium treatment involves the formation of a protective oxide film on the Al surface by reducing Cr(VI) to various Cr(III) compounds, which form a soft gel-like mixture along with metallic oxidation of the surface to Al oxide (Kulinich and Akhtar, 2012).

This study provides comprehensive details on the processes involved in each method, along with chemical characterization analysis. The chemical structural changes were evaluated using total reflectance infrared (ATR-FTIR) spectroscopy and scanning electron microscopy (SEM). Subsequently, RN binding experiments were conducted for two elements: ^{152}Eu and ^{241}Am. Radiological characterization was carried out using an autoradiography imager and a liquid scintillation counter device. Autoradiography imaging analysis was used to assess the uniformity of the sources, and liquid scintillation counting was employed to determine the radioactivity levels of the produced sources. These results contribute to the development of reliable and accurate radioactive sources for calibration.

2. Experimental

2.1. Materials

Surface sources were prepared using 25 cm^2 Al foils cut from a 0.03 mm thick Al foil (99.5%, Neyco). The sulfonation method included hydrogen peroxide (30% H_2O_2, Sigma–Aldrich), 3-mercaptopropyl trimethoxysilane (95% MPTS, $HS(CH_2)_3Si(OCH_3)_3$, Sigma-Aldrich) and acetone (99.5%, Carlo Erba). The manganese oxide treatment involved potassium permanganate (≥99.0%, $KMnO_4$, Prolabo) and sodium hydroxide (1 M NaOH, Sigma-Aldrich). The chromium oxide method involved potassium dichromate (≥99.0% $K_2Cr_2O_7$, Merck) and sulfuric acid (98%, H_2SO_4, Merck).

A solution of ^{152}Eu in 1 M HCl, with 0.2 μg g^{-1} of Eu as $Eu(NO_3)_3$, of activity (22.01 ± 0.07) kBq•g^{-1} (reference date: 28/11/2022), and a solution of ^{241}Am in 1 M HCl (no carrier, (31.06 ± 0.14) kBq•g^{-1}, same date), were used.

2.2. Functionalisation methods

The Al foils were cut before each experiment. Functionalisation solutions were prepared following the conditions shown in Table 1.

The concentrations of the chemicals in the functionalisation solution were taken from the literature (Boxus et al., 1996; Chen et al., 2010; Danilidis et al., 2007; Siau et al., 2004). The sulfonation treatment was adapted to our study with an additional pre-treatment step applied in boiling water (Chen et al., 2010). Several steps followed to immobilise the sulfonic acid groups on the Al foil. In all cases, the bare Al foil was cleaned in an ultrasonic bath consecutively with DI water, acetone and ethanol. To release OH bonds from the surface, boiling water and H_2O_2 treatments were performed: after drying, the sample was immersed in boiling water for 5 min and dried vertically at room temperature (Özkanat et al., 2012); the dried sample was then immersed in an H_2O_2 solution for 2 h and subsequently rinsed with DI water. The sample was then placed in an oven at 100 °C to dry overnight. Then, the Al foil was dipped in a MPTS/acetone solution (volume fraction of 1:100) for 3 h or 20 h, and then rinsed with acetone. Finally, Al foil was placed to cure in an oven at 100 °C. After this step, we expect thiol functional groups to be grafted onto the surface. Then, the Al foil was immersed in a 30% H_2O_2 solution for over 1 day to oxidise the thiol end-groups into sulfonic acid groups (Chen et al., 2010), and dried at room temperature.

The treatment of manganese oxide was carried out under acidic and basic conditions, following the literature (Boxus et al., 1996; Danilidis et al., 2007; Siau et al., 2004), with adjustments made to the temperature and duration of the reaction. The bare Al foil was used without any pre-treatment. The foils were immersed in a $KMnO_4$-NaOH solution. The H2 and H4 s had different molar concentrations of $KMNO_4$ (Table 1), and were prepared by dipping in the functionalisation solution. This allowed us to determine the effect of the concentration of $KMNO_4$ on the functionalisation reaction. For J3, the molar concentration was kept at 0.34 M with a longer duration (15 min), whereas H3 had a duration of 60 min, to study the effect of the duration of the reaction. All these methods were performed in basic conditions. An additional method was tested for I1 in acidic condition with 0.27 M $KMnO_4$ and 18 M H_2SO_4, to observe the impact of the pH of the functionalisation solution on the stability of the formed layer during radionuclide binding experiments (always under acidic conditions).

The chromium oxide method was performed under acidic conditions: the bare Al foil was immersed in a solution of 0.5 M $K_2Cr_2O_7$ and 18 M H_2SO_4 for durations of 10 and 60 min.

Both side of the samples were coated by horizontal immersion in the solutions for each method. After deposition, the samples were removed from the solution, washed under a gentle flow of distilled water, and left to dry vertically overnight at room temperature.

Table 1
Experimental conditions for the functionalisation step.

	Chemical	Solvent	Duration	$T_{functionalization}$(°C)
G3	0.05 mM MPTS	Acetone	3 h	22
E8	0.05 mM MPTS	Acetone	20 h	22
H2	0.1 M $KMnO_4$	1 M NaOH	Dipped	22
H4	0.34 M $KMnO_4$	1 M NaOH	Dipped	50
J3	0.34 M $KMnO_4$	1 M NaOH	15 min	50
H3	0.34 M $KMnO_4$	1 M NaOH	60 min	50
I1	0.27 M $KMnO_4$	18 M H_2SO_4	60 min	50
I3	0.5 M $K_2Cr_2O_7$	18 M H_2SO_4	10 min	50
I2	0.5 M $K_2Cr_2O_7$	18 M H_2SO_4	60 min	50

2.3. Surface characterisation

Attenuated total reflection Fourier transform infrared spectroscopy (ATR-FTIR) was used to identify the chemical functions on the sample surfaces. A Q Platinum-ATR (Bruker) device was used, and the spectra were obtained by using 128 scans from 600 to 4000 cm^{-1}, scan rate of 2.0 cm^{-1}).

The morphology of the functionalised Al surfaces was examined by scanning electron microscopy (SEM) using an XL40 (Thermo Fisher) microscope. Secondary electrons imaging was used to obtain the images.

2.4. Radionuclide binding experiments

In all experiments, gravimetric dilutions were performed to keep the traceability. The radionuclide binding medium was prepared by mixing ultrapure water, 1 M HCl (to reach pH 2), and a stock solution of radionuclide. Ultrapure water and HCl solutions were weighed using a Mettler-Toledo XPE504 balance (range of 500 g, resolution of 0.1 mg) and the radioactive solution was weighed using the pycnometer method (Lourenço and Bobin, 2015) and a Mettler-Toledo MT5 microbalance (range 5 g, resolution of 1 μg). The beakers were agitated and homogenize after the addition of each component. Finally, the Al foils were immersed in the RN binding medium for a certain amount of time. For both RNs, the total amount of elements (stable and active) in solution was kept as close as to compare the fixation yields, as shown in Table 2. A reference solution was prepared for each RN using the same

Table 2
The parameters of radionuclide binding experiment.

RN	Stable/Active element ratio	Total amount of element in solution (picomol)
^{152}Eu	~57	~0.4
^{241}Am	No carrier	~0.5

components as the sample solutions, without immersing any samples.

2.5. Radiological characterisations

Liquid Scintillation Counting (LSC) analysis was performed using a TRICARB 2900 TR (PerkinElmer). The sources were prepared by mixing 1 mL of samples with 10 mL of scintillator (Ultima Gold, Perkin Elmer) and measured for 15 min each. The overall activity per sample was approximately 20 Bq, and a blank sample, prepared with Eu carrier solution was used to correct the data.

The functionalised Al foils were immersed in the radionuclide (RN) solution to allow the binding of RN to the surface as shown in Fig. 1. LSC was performed to measure radioactivity remaining in the RN binding mixture, and samples were taken at 2-h intervals from this solution. The maximum fixation yield (Y) was calculated using Equation (1) at the moment when the fixation yield was maximum. $(CPS/g)_{sample}$ and $(CPS/g)_{ref}$ represents the count per second per gram of the sample and of the reference solution (without any sample), respectively.

$$Y = \frac{\left(\frac{CPS}{g}\right)_{ref} - \left(\frac{CPS}{g}\right)_{sample}}{\left(\frac{CPS}{g}\right)_{ref}} \quad (1)$$

The calculations were performed assuming that all RN atoms were bound to the Al surface. This assumption was verified by ensuring that the RN in solution did not attach to the walls of the glass beakers despite contact for several days. The samples spiked with ^{152}Eu were kept in the RN mixture for up to 24 h or 48 h, while the one spiked with ^{241}Am (J3) was kept for 4 h.

The uniformity of the sources was analysed using BAS-MS Fujifilm imaging plates and a GE Healthcare Amersham Typhoon scanner, with a resolution of 100 μm. The sources were placed on the screen with close contact for 72 h and imaged with the scanner after exposure. The images obtained were analysed using the software OptiQuant.

Each pixel of an autoradiography image has a numerical value that is proportional to the amount of radiation detected in that area during exposure. To determine the uniformity of the source, the sources should be divided into equal-shaped portions, with each portion being about 10 cm^2 or less (ISO 2022), and the sum of the pixels in one area is compared to the sum of the pixels in the other areas. The samples (25 cm^2) were divided into 9 square portions (3 × 3, each measuring 2.7 cm^2) and 4 square portions (2 × 2, each measuring 6.25 cm^2). The uniformity of a source is expressed as 1 minus the standard deviation of the surface emission rates (σ_n) of each individual portion of the entire reference measurement standard divided by the mean value of these emission rates (n) as given in Equation (2):

$$\left(1 - \frac{\sigma_n}{n}\right) \times 100\ (\%) \quad (2)$$

Two sets of exposures were performed to observe the uniformity of the prepared sources. In the first set, the radioactive sources were kept in close contact with the photosensitive screen for 72 h. Due to the dual alpha and gamma emissions of ^{241}Am and the dual beta and gamma emissions of ^{152}Eu, the obtained images show the sum of the distribution of all types of radiation. Therefore, an additional exposure experiment was performed for the chosen sources, using a masking plate between the source and detector screen. For the ^{152}Eu sources, an Al foil (0.03 mm thick) was placed to attenuate most of the beta particles emitted by the source, while for the ^{241}Am source, a sheet of paper was used to stop alpha particles.

3. Results and discussion

3.1. Chemical characterisation

3.1.1. Infrared spectroscopy

To identify the chemical functions of the functionalised Al surfaces, infrared spectroscopy (ATR-FTIR) was performed on bare Al foil, a sulfonated sample, a manganese oxide coated sample and a chromium oxide coated sample. In the case of bare Al foil (Fig. 2a), a low-intensity IR band was observed between 940 and 960 cm^{-1}, attributed to the Al-O stretching vibration due to Al_2O_3 present on the surface (Danilidis et al., 2007). However, after the functionalisation treatments, this peak was no longer observed in the spectra. The disappearance of this peak can be attributed to the presence of high-intensity peaks in the spectra of the modified Al foil, which may obscure the underlying peak. Furthermore,

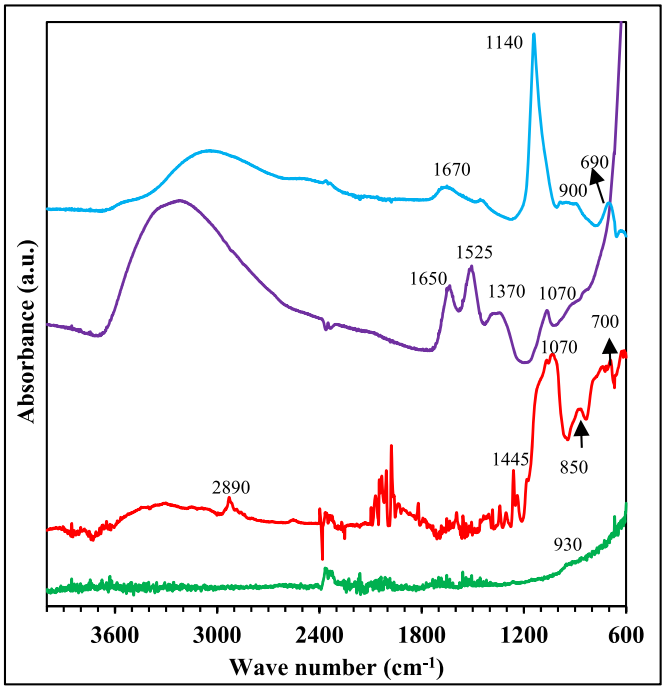

Fig. 2. ATR-FTIR spectroscopy of the functionalised Al foils: (a) Bare Al foil, (b) E8-Sulfonation coating, (c) H3-J3-Manganese oxide coating, (d) I2-Chromium oxide coating.

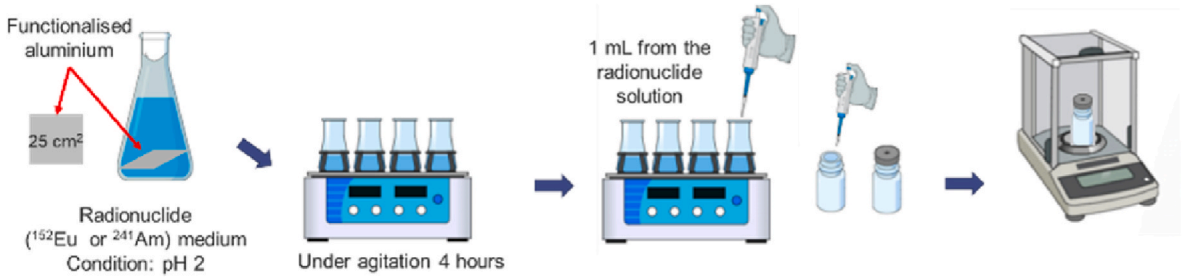

Fig. 1. The setup of the radionuclide binding experiment.

the absence of other specific peaks in the bare Al spectrum indicates that there is no detectable organic coating on the surface (Boxus et al., 1996).

The sulfonated sample (E8, Fig. 2b) exhibits a broad band from 3700 to 3400 cm^{-1} attributed to the stretching vibrations of hydroxyl groups (Lourenço and Bobin, 2015). The bands observed at 2890 cm^{-1} correspond to the C-H (CH_2 or CH_3) chemical bonds (Boxus et al., 1996). The IR band near 1070 cm^{-1} is attributed to the monohydrate Al-OH bending, and also corresponds to the SO_3^- stretching (Özkanat et al., 2012). Also the absorption band in the range 1100-1000 cm^{-1} indicates the formation of Al-O-Si and Si-O-Si bonds with the underlying substrate and within the coating, respectively. Due to molecular weights of Al and silicon being close to each other, their respective stretching vibrations can overlap in this region of the spectrum. Additionally, the bond at approximately 850 cm^{-1} is attributed to the stretching of siloxane, indicating the presence of Si-O-Si bonds. These results demonstrate that sulfonated groups are successfully attached to the Al surface as illustrated in Fig SI1.

Treatment with the $KMnO_4$ solution (J3, Fig. 2c) introduces a broad absorption band in the region of 3100–3600 cm^{-1} indicating asymmetric and symmetric –OH bond stretching vibrations (Siau et al.,

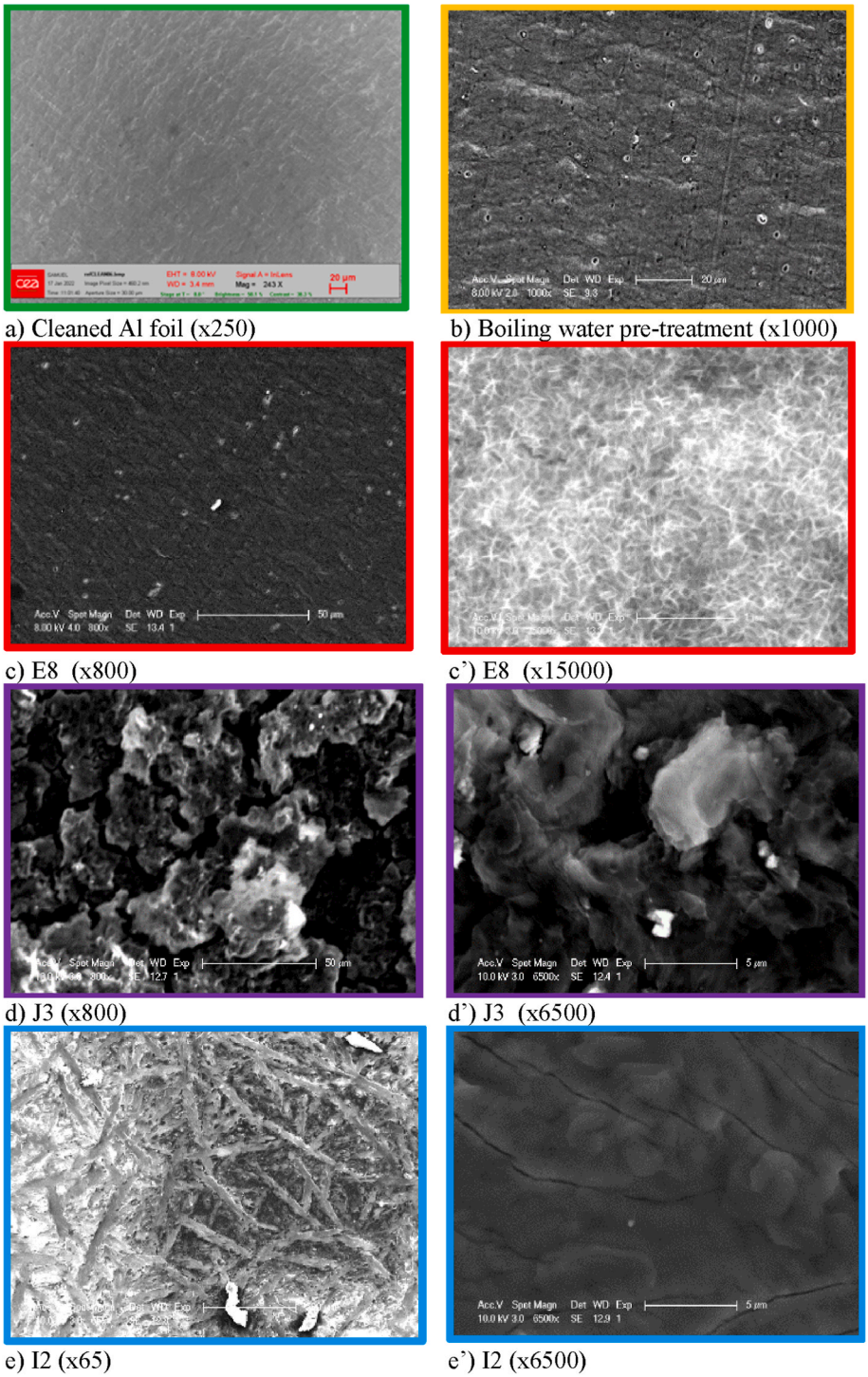

Fig. 3. SEM images of (a) bare Al foil, (b) boiling water treated sample, (c) and (c') E8 (Sulfonation), (d) and (d') J3 (Mn oxide coated), and (e) and (e') I2 (Cr oxide coated). The numbers written in brackets indicate the magnification of the images.

2005). The bands at 1370, 1525 and 1650 cm^{-1} correspond to O-H bending vibrations (Zheng et al., 2013). The band observed at 660 cm^{-1} is attributed to the stretching vibration of the Mn-O bonds (del Olmo et al., 2022; Kang and Kim, 2020; Zheng et al., 2013). Finally, it can be concluded that all observed peaks indicate the formation of a manganese oxide coating on the Al surface.

The spectrum of the sample functionalised with $K_2Cr_2O_7$ (Fig. 2d) also shows a broad absorption band in the region of 3100–3600 cm^{-1} which can be attributed to the stretching bond vibration mode of -OH bonds similar to the $KMnO_4$ treatment (Özkanat et al., 2012; Siau et al., 2004). The peak at 1636 cm^{-1} indicates HOH bending of water molecules bound in the chromium film (Xia and McCreery, 1998). The fingerprint region has a high-intensity peak at 1140 cm^{-1}, which is assigned to the Cr(V) species (Vuurman et al., 1993; Xia and McCreery, 1998) . The shoulder around 960 cm^{-1} indicates a Cr(VI)-O vibration, which can be due to the Al/Cr mixed oxide or Cr mixed oxide. This also showed that a Cr(VI)-O coating was present on the surface of the Al foil.

ATR-FTIR spectroscopy showed that functionalisation methods resulted in changes in the chemical composition of the surface and the formation of new bonds with the underlying substrate and within the coating.

3.1.2. Scanning electron microscopy analysis

After undergoing functionalisation, the samples displayed distinct surface appearances and colours. E8 (Sulfonated) showed whitish traces on the surface, while J3 (Mn oxide coated) appeared brownish, and I2 (chromate oxide coated) exhibited a greyish coating.

The morphologies of four selected samples (bare Al foil, sulfonated E8, manganese oxide coated J3 and chromium oxide coated I2) were examined using scanning electron microscope (SEM). The topography of the samples varied significantly according to the method used. The SEM image of the bare Al foil (Fig. 3a) did not exhibit any specific features, which indicates that the surface was clean and there were no organic residues present. After the boiling water treatment, micro and nano-particles appeared, as well as some porosity (Fig. 3b). E8 (Fig. 3c) exhibited bright particle sizes of up to 7 μm. The-high magnification image (Fig. 3 c') also revealed the presence of nanoscale needle-like structures evenly distributed all over the surface.

J3 (Mn oxide coated, Fig. 3 d and d') shows a coating with open pores on the entire surface. The high-magnification image revealed that, in addition to the globule structure, white particles were observed with sizes up to 1.5 μm.

The I2 sample (Cr oxide coated Fig. 3 e and e') had a needle-like structure on its surface. These structures are similar in size, shape, and distribution with sizes up to 50 μm.

3.2. Radiological characterisation

3.2.1. Liquid scintillation counting analysis

The following section presents the analysis from the LSC experiments conducted in this study. Table 3 indicates the maximum fixation yield that was achieved in the radionuclide (RN) binding experiment, and the corresponding duration of the immersion of the sample.

Samples G3 and E8 were produced by sulfonation, G3 after 3 h and E8 after 20 h of reaction (Table 1). The LSC results revealed that both samples exhibited maximum fixation yields around 15% (Table 3). For G3, the maximum fixation yield was reached after 1 h, while E8 achieved its maximum after 48 h. It could be due to the fact that fixed RNs can be released from the surface, or to the alteration of the sulfonation coating in the RN binding medium. On the other hand, E8 achieved its maximum fixation yield after 48 h, which could signify that the longer duration of sulfonation can improve the stability of the coating in an acidic medium. An example of the variation of the fixation yield (for G3) with exposure time is given in Fig SI2.

H2 and H4 were produced by dipping the foils in a manganese oxide solution, using a different concentration of $KMnO_4$ solution (Table 1).

Table 3
Maximum fixation yields of each sample.

Sample	RN	Functionalisa-tion duration	Maximum fixation yield with standard ($k = 1$) uncertainty	t of max fixa-tion
G3	^{152}Eu	3 h Sulfonation	(15.0 ± 2.7)%	1 h
E8	^{152}Eu	20 h Sulfonation	(12.7 ± 2.5)%	48 h
H2	^{152}Eu	Dipped Mn oxide	(4.6 ± 2.8)%	2 h
H4	^{152}Eu	Dipped Mn oxide	(6.6 ± 2.8)%	2 h
J3-Am	^{241}Am	15 min Mn oxide	(70.0 ± 2.6)%	4 h
H3	^{152}Eu	60 min Mn oxide	(7.6 ± 2.8)%	4 h
I1	^{152}Eu	60 min Mn oxide	-(3.2 ± 2.9)%	2 h
I3	^{152}Eu	10 min Cr oxide	-(1.6 ± 2.9)%	2 h
I2	^{152}Eu	60 min Cr oxide	(18.8 ± 2.7)%	2 h

The fixation yields of both the samples were found to be close (Table 3). The one with the highest Mn concentration is slightly higher but in both cases, the fixation yields remain low, possibly due to a too short contact time between the samples and the $KMnO_4$ solution, to produce a Mn oxide coating that can efficiently bind to RN.

The effect of the functionalisation duration was examined by comparing the H4 (dipped) and H3 (60 min) samples (Table 1), and the results showed that the maximum fixation yield was not affected by that parameter, confirming that this functionalisation method allows to reach only a moderate fixation yield of RN.

I1 was the only formed in acidic conditions for the manganese oxide treatments.

In the analysis of I1 and I3 samples, the fixation yield calculated using Eq. (1) was negative (Table 3), indicating an increase of the activity of the RN binding solution over time. As the evaporation of the solutions was regularly monitored, the observed increase can potentially be attributed to uncertainties inherent in the measurement process, and those results lead us to conclude that no fixation of RN was observed for these samples.

Chromium oxide treatments with different functionalisation durations, namely I3 (10 min) and I2 (60 min) (Table 1), were also compared. The results revealed that the functionalisation duration has an impact on the fixation yield for chromium treatment. The I3, which was treated for 10 min, had an increase in the radioactivity level within the uncertainty values, as explained above. However, I2 had a maximum fixation yield of 18.8%. This suggests that a longer functionalisation duration led to a higher fixation yield.

J3 exhibited the highest fixation yield compared to all other samples, while the functionalisation method used was Mn oxide, similar to samples H3 and H4 (Table 1). For the Eu solution used for the RN binding experiment of H3 and H4, the stable/active element ratio was 57, whereas no carrier element was present in the solution for the Am sample J3. This large amount of stable Eu in solution contributes to occupy fixation sites on the surface (as illustrated in Fig. 4), resulting in lower fixation yields, despite the nearly identical total amount of elements in the solution.

The maximum activities of the samples showing a significant fixation yield are given in Table 4. The ^{152}Eu surface sources produced using various methods had maximum activities of about a few Bq•cm^{-2}. The ^{241}Am surface sources produced using manganese oxide coating method had the highest activity 25.09 ± 0.92 Bq•cm^{-2}.

Although this activity level is above the low-level radioactive source threshold of 0.2 Bq•cm^{-2}, it can be easily adjusted by adapting the radioactivity level of the spiking solution in which the sample is

Fig. 4. Illustration of immersion of functionalised Al foils in ^{152}Eu and ^{241}Am solutions.

Table 4
Maximum activity of the Al-functionalised surface sources.

Samples	RN	%LSC activity decrease	Maximum activity bound, standard uncertainty ($k = 1$) (Bq•cm^{-2})
G3 Sulfonation	^{152}Eu	(15.0 ± 2.7)%	3.29 ± 0.59
E8 Sulfonation	^{152}Eu	(12.7 ± 2.5)%	2.90 ± 0.62
I2 Cr oxide	^{152}Eu	(18.8 ± 2.7)%	3.69 ± 0.52
H3 Mn oxide	^{152}Eu	(7.6 ± 2.8)%	1.66 ± 0.61
J3 Mn oxide	^{241}Am	(70.0 ± 2.6)%	25.09 ± 0.92

immersed.

3.2.2. Autoradiography imaging

The main assumption underlying the LSC counting analysis was that the differences between each sampling interval indicated the amount of RN fixed onto the Al foil. In addition, the absence of fixation of the activity on the walls of the beakers was checked. In this section phosphor imaging autoradiography images were used to confirm the presence of radionuclides attached onto the surfaces, and to assess the uniformity of the radionuclide distribution on the surface.

In order to de-couple the image coming from the dual beta and gamma emissions of ^{152}Eu and alpha and gamma emissions of ^{241}Am, the sources were exposed to a film with and without a mask. The uniformity of the gamma photons emitted from the masked sources and the uniformity of the sources are listed in Table 5. The uniformity of the masked sources did not exhibit any significant changes compared with the source itself. These slight differences may be within the uncertainty values.

The impact of the grid size was also investigated (Table 6). The results indicate that changing the grid size does not have an impact on uniformity values.

Fig. 5 presents the autoradiography images of the samples G3, E8, I2 and J3 after 72 h of exposure, with a 3 × 3 grid size.

Notable differences are observed in the autoradiography images of samples G3 and E8. The image of E8 (Fig. 5b) showed higher RN attachment compared to G3 (Fig. 5a). This difference is coherent with the LSC results showing that although both samples reach a similar maximum fixation yield (Table 3), the yield of G3 increased afterwards, leading to less activity being bound on the surface. This may be attributed to the different duration of the functionalisation treatment (3 h for G3 and 20 h for E8), the longer functionalisation time producing a coating that is more resistant to the RN binding solution. The uniformity of E8 was 75%, with the majority of the activity concentrated along one edge of the sample, forming a triangular shape. This shape observed in the radioactive emission pattern is consistent with the white traces on E8, which could indicate the location were functionalisation occurred. Therefore, it is plausible that two factors contribute to the observed pattern in the autoradiography image: the distribution of sulfonation groups and the distribution of radioactivity on the Al surface. The folding of the Al foils may have played a role in these effects.

Table 6
The uniformity values for two different grid sizes.

		Uniformity	
Method	RN	2 × 2	3 × 3
G3 Sulfonation	^{152}Eu	86%	81%
E8 Sulfonation	^{152}Eu	72%	75%
I2 Cr oxide	^{152}Eu	61%	58%
J3 Mn oxide	^{241}Am	93%	92%

I2 has 58% of uniformity with the emitted particles primarily located on one side of the sample (Fig. 5c).

The J3 sample exhibits the highest degree of uniformity (93%), with a high radioactivity fixation yield at (70.0 ± 2.6)%. Autoradiography image indicates the successful RN attachment over the entire surface, although a slight disparity was observed between the center and the edges (Fig. 5d). This discrepancy may be due to experimental conditions, such as rotational movement of the agitator during the manganese coating process, which could impact the distribution of the coating on the surface.

4. Conclusion

This study aimed to produce flexible and traceable surface sources for alpha and beta emitters. Three distinct methods with MPTS, $KMnO_4$ and $K_2Cr_2O_7$ chemicals were used to attach trivalent radioactive lanthanide or actinide elements on the surface with strong chemical bonds. Various parameters such as the reaction duration, molar ratio and reaction temperature were evaluated. Chemical analyses (ATR-FTIR and SEM) proved the successful functionalisation of the Al surfaces. Additionally, the results of the radiological characterisations (LSC and autoradiography) showed that J3 (manganese coating-Am spiked) had the highest fixation yield of (70.0 ± 2.6) % with a surface activity of (25.07 ± 0.92) Bq•cm^{-2}. This sample also has the highest uniformity value among the others (92%), which complies with the ISO8769

Table 5
The uniformity values of the sources with and without masking plate.

Method	RN	Masking plate	Overall uniformity	Uniformity of emitted photons
G3 Sulfonation	^{152}Eu	Al foil (0.03 mm)	81%	82%
E8 Sulfonation	^{152}Eu	Al foil (0.03 mm)	75%	79%
I2 Cr oxide	^{152}Eu	Al foil (0.03 mm)	58%	58%
J3 Mn oxide	^{241}Am	Sheet of paper	92%	94%

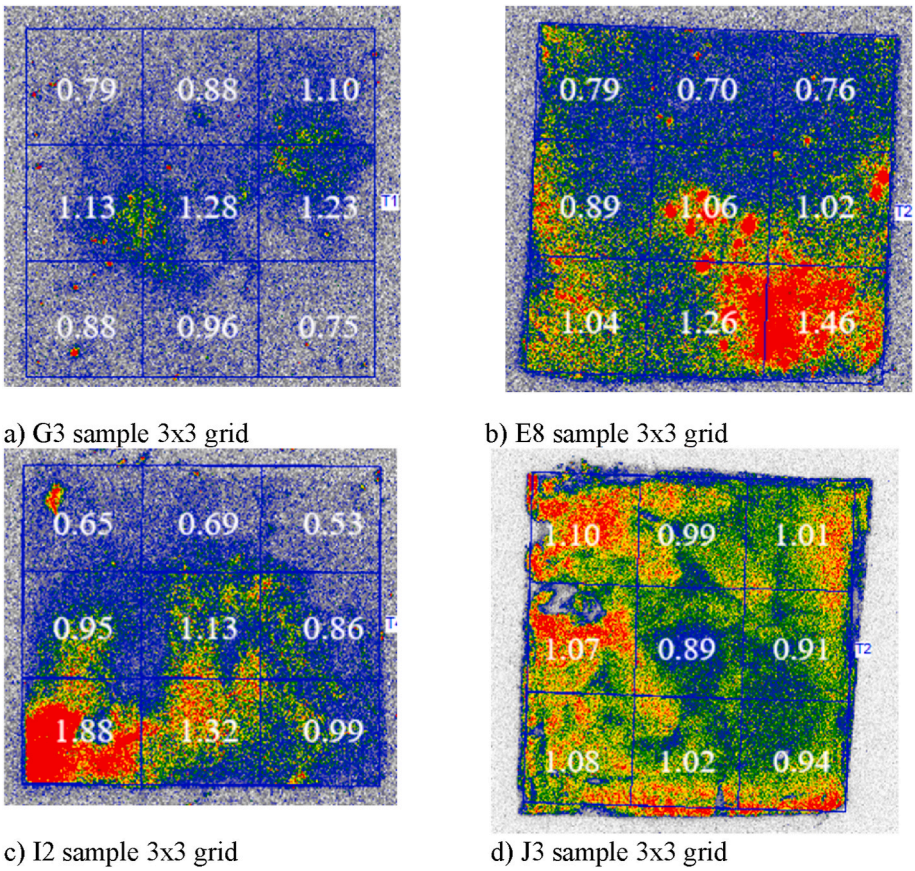

Fig. 5. Phosphor imaging autoradiography images (a) G3 sulfonated sample ^{152}Eu, (b) E8 sulfonated sample ^{152}Eu, (c) I2 Cr oxide sample ^{152}Eu, d) J3 Mn oxide sample ^{241}Am. All the samples measure 5 × 5 cm^2, and were exposed for 72 h, G3, E8 and I2 in one film and J3 in another.

standard (ISO 2022). Future studies could focus on using ^{244}Cm, to obtain pure alpha emitter sources. To improve the uniformity, increasing the thickness of the Al foil to 0.3 mm can be considered to prevent folding at the edges and maintain the Al's structure even in harsh experimental functionalisation conditions. Non-contamination tests will be performed to assess the contamination of the sources. We managed to successfully produce traceable surface sources with a range of radioactivity levels from 2 to 25 Bq•cm^{-2}. These values are easily adjustable by adapting the radioactive level of the spiking solution used for sample immersion.

CRediT authorship contribution statement

D. Tüzün: Writing – review & editing, Writing – original draft, Methodology, Investigation, Formal analysis, Data curation. **L. Chambon:** Writing – review & editing, Validation, Supervision, Methodology, Formal analysis. **Y. Kergadallan:** Methodology, Formal analysis. **V. Lourenço:** Writing – review & editing, Validation, Supervision, Resources, Methodology, Funding acquisition, Conceptualization.

Declaration of competing interest

The authors declare that they have no known competing financial interests or personal relationships that could have appeared to influence the work reported in this paper.

Data availability

Data will be made available on request.

Acknowledgements

We would like to thank Denis Doizi for providing access to the FTIR device, Pierre-François Orfila for his assistance and guidance with SEM imaging, and Stephanie Heinkele for conducting the liquid scintillation counting measurements. Their contributions were essential to the progress and outcomes of this research.

Appendix A. Supplementary data

Supplementary data to this article can be found online at https://doi.org/10.1016/j.apradiso.2023.111045.

References

Boxus, T., Deldime-Rubbens, M., Mougenot, P., Schneider, Y.-J., Marchand-Brynaert, J., 1996. Chemical assays of end-groups displayed on the surface of poly(ethylene terephthalate) (PET) films and membranes by radiolabeling. Polym. Adv. Technol. 7, 589–598.

Chambon, L., Tüzün, D., Bobin, C., Corbel, M., Lourenço, V., 2022. Development of alpha-emitting large area radioactive surface sources tailored for decommissioning. Nucl. Instrum. Methods Phys. Res. Sect. A Accel. Spectrom. Detect. Assoc. Equip. 1033, 166732.

Chen, Y.-F., Hu, Y.-H., Chou, Y.-I., Lai, S.-M., Wang, C.-C., 2010. Surface modification of nano-porous anodic alumina membranes and its use in electroosmotic flow. Sensor. Actuator. B Chem. 145, 575–582.

Danilidis, I., Davenport, A.J., Sykes, J.M., 2007. Characterisation by X-ray absorption near-edge spectroscopy of KMnO4-based no-rinse conversion coatings on Al and Al alloys. Corrosion Sci. 49, 1981–1991.

del Olmo, R., Mohedano, M., Matykina, E., Arrabal, R., 2022. Permanganate loaded Ca-Al-LDH coating for active corrosion protection of 2024-T3 alloy. Corrosion Sci. 198, 110144.

ISO, 2022. NF EN ISO 8769:2022, Measurement of Radioactivity - Alpha-, Beta- and Photon Emitting Radionuclides - Reference Measurement Standard Specifications for the Calibration of Surface Contamination Monitors. International Organization for Standardization, Geneva.

Kang, J.-K., Kim, S.-B., 2020. Synthesis of quaternized mesoporous silica SBA-15 with different alkyl chain lengths for selective nitrate removal from aqueous solutions. Microporous Mesoporous Mater. 295, 109967.

Kulinich, S.A., Akhtar, A.S., 2012. On conversion coating treatments to replace chromating for Al alloys: recent developments and possible future directions. Russ. J. Non-Ferrous Metals 53, 176–203.

Lourenço, V., Bobin, C., 2015. Weighing uncertainties in quantitative source preparation for radionuclide metrology. Metrologia 52, S18.

Özkanat, Ö., Salgin, B., Rohwerder, M., Mol, J.M.C., de Wit, J.H.W., Terryn, H., 2012. Scanning kelvin probe study of (Oxyhydr)oxide surface of aluminum alloy. J. Phys. Chem. C 116, 1805–1811.

Siau, S., Vervaet, A., Schacht, E., Calster, A.V., 2004. Influence of chemical pretreatment of epoxy polymers on the adhesion strength of electrochemically deposited Cu for use in electronic interconnections. J. Electrochem. Soc. 151, C133.

Siau, S., Vervaet, A., Schacht, E., Degrande, S., Callewaert, K., Van Calster, A., 2005. Chemical modification of buildup epoxy surfaces for altering the adhesion of electrochemically deposited copper. J. Electrochem. Soc. 152, 136.

Vuurman, M.A., Wachs, I.E., Stufkens, D.J., Oskam, A., 1993. Characterization of chromium oxide supported on Al_2O_3, ZrO_2, TiO_2, and SiO_2 under dehydrated conditions. J. Mol. Catal. 80, 209–227. https://doi.org/10.1016/0304-5102(93)85079-9.

Xia, L., McCreery, R.L., 1998. Chemistry of a chromate conversion coating on aluminum alloy AA2024-T3 probed by vibrational spectroscopy. J. Electrochem. Soc. 145, 3083. https://doi.org/10.1149/1.1838768.

Zheng, M., Zhang, H., Gong, X., Xu, R., Xiao, Y., Dong, H., Liu, X., Liu, Y., 2013. A simple additive-free approach for the synthesis of uniform manganese monoxide nanorods with large specific surface area. Nanoscale Res. Lett. 8, 166. https://doi.org/10.1186/1556-276X-8-166.